Electrochemical Promotion by Sodium of the Rhodium−Catalyzed Reduction of NO by Propene: Kinetics and Spectroscopy

ARTICLE *in* THE JOURNAL OF PHYSICAL CHEMISTRY B · FEBRUARY 2001

Impact Factor: 3.3 · DOI: 10.1021/jp003269d

Electrochemical Promotion by Sodium of the Rhodium-Catalyzed Reduction of NO by Propene: Kinetics and Spectroscopy

Federico J. Williams, Alejandra Palermo, Mintcho S. Tikhov, and Richard M. Lambert*

Department of Chemistry, University of Cambridge, Cambridge CB2 1EW, England

Received: September 13, 2000; In Final Form: December 11, 2000

The catalytic performance of rhodium thin films in contact with the solid electrolyte Na β''-alumina can be greatly enhanced by electrochemical promotion. In the reduction of NO by propene, increases in overall activity by a factor of 2.4 can be achieved accompanied by a gain in nitrogen selectivity from 45% to 82%. These improvements are most pronounced under reducing conditions and are unaffected by deliberate addition of CO_2. XPS data show that the effect is due to reversible transport of Na between the solid electrolyte and the metal film catalyst whose potential, measured with respect to a reference electrode, determines the sodium coverage. Catalytic promotion is due to the Na-induced dissociation of NO, the key reaction-initiating step. Under reaction conditions, the sodium is present as carbonate, some of which is in the form of 3D crystallites. Comparison with corresponding data obtained with conventional dispersed Rh/γ-alumina catalysts shows that Na promotion of the latter is due to the effect of alkali on the surface chemistry of the metal component; effects on the support must be negligible.

1. Introduction

Current automotive catalytic converters employ various combinations of Pt, Pd, and Rh for the simultaneous removal of NO_x, CO, and unburned hydrocarbons.[1,2] Of these metals, rhodium is the key component with respect to NO_x reduction due to its high activity for the dissociative chemisorption of NO,[3] which process seems likely to play an important role in the catalytic reduction of NO_x. Even so, Rh-based catalysts exhibit less than 100% selectivity toward nitrogen formation, substantial amounts of N_2O being produced as well. Although N_2O emission is not yet covered by legislation, it seems unlikely that this situation will persist as nitrous oxide is a powerful greenhouse gas. Attempts have therefore been made to improve the selectivity of Rh catalysts by doping either the Rh component itself,[4] or the support material.[5] Interpretation of the observed effects remains, however, largely speculative. Recently we showed that the catalytic performance of Rh particles supported on γ-alumina in the reduction of NO_x by propene could be greatly improved by Na promotion.[6] Though encouraging, a full understanding of these results is impeded by one of the most difficult problems that arises in studies of heterogeneous catalysis by dispersed metal systems, namely, how is the promoter species distributed between the metal component and the support phase?

Electrochemical promotion (EP) of thin film metal catalysts offers a way forward.

The technique entails electrochemical pumping of ions from a solid electrolyte to the surface of a porous, catalytically active metal film with which it is in contact. Here we use Na β''-alumina (a Na^+ conductor) as the solid electrolyte. Under forward bias (catalyst working electrode negative relative to counter electrode) Na^+ ions are transported to the working electrode where they are discharged at the metal electrode/solid electrolyte/gas three-phase boundary. It is proposed that the resulting Na species spills over onto the surface of the metal catalyst, strongly altering its electronic properties, including its work function. The adsorption enthalpies of adsorbed species and activation energies of reactions involving these species should therefore be affected. Thus we have a means of in situ control of alkali promoter levels on the working metal catalyst and the interpretation of results is freed from ambiguities associated with possible effects of the alkali on the support phase. Here we show that EP induces selectivity and activity improvements commensurate with those found with Na-promoted conventional dispersed Rh catalysts and a mechanism for Na promotion of Rh is proposed. XPS data illuminate the mode of action of EP. They also reveal the chemical identity of the Na-containing promoter phase and provide some insight into its morphology.

2. Experimental Methods

EP samples for catalytic testing and spectroscopic analyses were prepared by depositing a rhodium metal film on one face of a Na β''-alumina wafer: this constituted the catalyst (working electrode). Gold counter and reference electrodes were deposited on the other face, all three electrodes being deposited by DC sputtering of Rh or Au in argon. These EP samples were characterized by XRD, XPS, and surface area measurements, as discussed in an earlier publication.[7] The rhodium surface area was estimated using the CO methanation technique developed by Komai et al.[8] This method makes use of a sensitive FID detector to monitor the conversion of chemisorbed CO to methane on the exposed metal sites. On the basis of a 1:1 CO-to-surface metal atom ratio, this yields a surface area equivalent to 0.1 μmol of Rh ($\sim$ 37.6 cm^2).

Rate data were acquired in a well-mixed reactor operated at atmospheric pressure. The EP sample was suspended in the reactor with all electrodes exposed to the reactant gas mixture. Inlet and exit gas analysis was carried out by a combination of on-line gas chromatography (Shimadzu-14B; molecular sieve

* Corresponding author. Tel: 44 1223 336467. Fax: 44 1223 336362. E-mail: RML1@cam.ac.uk.

10.1021/jp003269d CCC: $20.00
Published on Web 01/25/2001

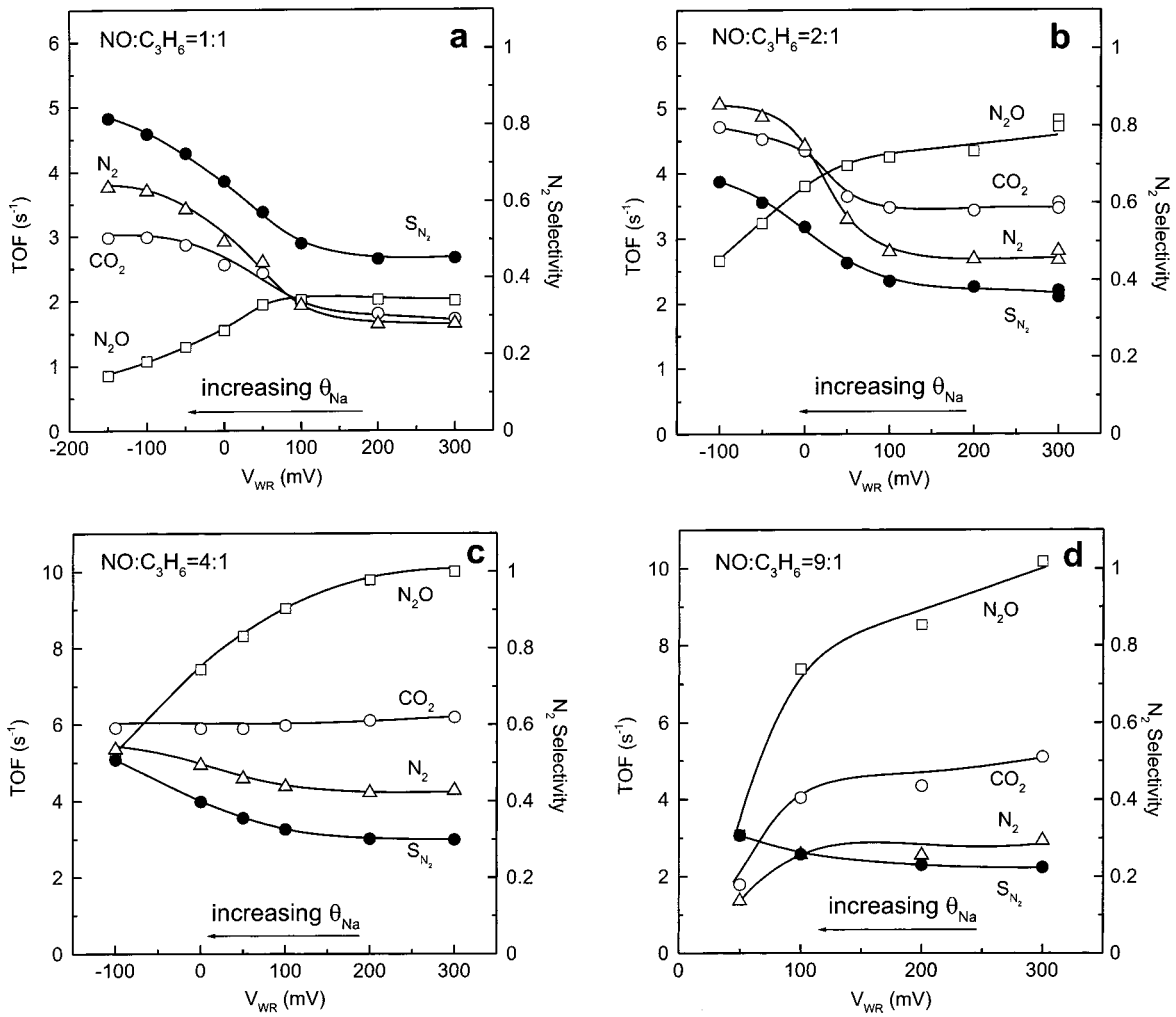

Figure 1. Effect of catalyst potential (V_{WR}) on CO_2, N_2, N_2O formation rates and the nitrogen selectivity at 623 K for different NO and propene partial pressures. (a) $P^0(NO) = 1$ kPa, $P^0(C_3H_6) = 1$ kPa. (b) $P^0(NO) = 2$ kPa, $P^0(C_3H_6) = 1$ kPa. (c) $P^0(NO) = 4$ kPa, $P^0(C_3H_6) = 1$ kPa. (d) $P^0(NO) = 9$ kPa, $P^0(C_3H_6) = 1$ kPa.

13X and Haysep-N columns) and on-line mass spectrometry (Balzers QMG 064). N_2, N_2O, CO, CO_2, and C_3H_6 were measured by gas chromatography, and NO was monitored continuously by mass spectrometry after performing the necessary calibrations. NO (Distillers MG) and C_3H_6 (Distillers MG) were diluted in ultrapure He (99.996%) and fed to the reactor by mass flow controllers (Brooks 5850 TR). The total flow rate was kept constant in all experiments at 34×10^{-5} mol s^{-1} (500 cm^3(STP)/min). Reactant conversion was restricted to <15% in order to avoid mass transfer limitations. Control experiments were carried out in which the total flow was varied by a factor of 5 in order to verify that the observed changes in activity were indeed due to changes in actual surface reaction rates, unaffected by mass transfer limitations. Nitrogen and carbon mass balances always closed to within 5%.

A galvanostat−potentiostat (Ionic Systems) was used in order to maintain a given potential difference (V_{WR}) between the working and reference electrodes (potentiostatic mode). All experiments were carried out in potentiostatic mode by following the effect of catalyst potential, i.e., the Na coverage (θ_{Na}), on the reaction rates. XPS experiments were performed under UHV conditions (base pressure $<10^{-10}$ Torr) in a VG ADES 400 UHV spectrometer system equipped with a reaction cell. The EP sample was mounted on a manipulator that allowed translation between the reaction cell and the spectrometer chamber. Full details regarding sample mounting, manipulation, and data acquisition are given in an earlier publication.[9] Quoted binding energies are referred to the $Au4f_{7/2}$ emission at 83.8 eV from the grounded Au wire that formed the electrical connection to the Rh working electrode.

3. Results

3.1. Effect of Catalyst Potential on Reaction Rates. Figure 1a−d shows steady-state rate data for CO_2, N_2, and N_2O production as a function of V_{WR} at 623 K for different inlet pressures ($P^0(NO)$, $P^0(C_3H_6)$) of nitric oxide and propene, $P^0(NO) = 1$ kPa and $P^0(C_3H_6) = 1$ kPa (a), $P^0(NO) = 2$ kPa and $P^0(C_3H_6) = 1$ kPa (b), $P^0(NO) = 4$ kPa and $P^0(C_3H_6) = 1$ kPa (c), $P^0(NO) = 9$ kPa and $P^0(C_3H_6) = 1$ kPa (d). Under these conditions CO_2, N_2, N_2O, and H_2O were the only products. Accurate measurement of the water production rate was not possible due to partial condensation within the sampling system. However, the behavior of the H_2O rate was qualitatively the same as the CO_2 rate under all conditions. Rates are expressed as turnover frequency (TOF), i.e., molecules of product per Rh surface atom per second. Also shown in Figure 1 is the V_{WR} dependence of the nitrogen selectivity (S_{N_2}) defined as the ratio of nitrogen rate to the sum of the (nitrogen + nitrous oxide) rates. As can be seen from Figure 1a, decreasing V_{WR} (Na pumping toward the Rh catalyst) causes an increase in the rate of CO_2 and N_2 formation and a decrease in the N_2O production. This induces a remarkable increase in the nitrogen selectivity.

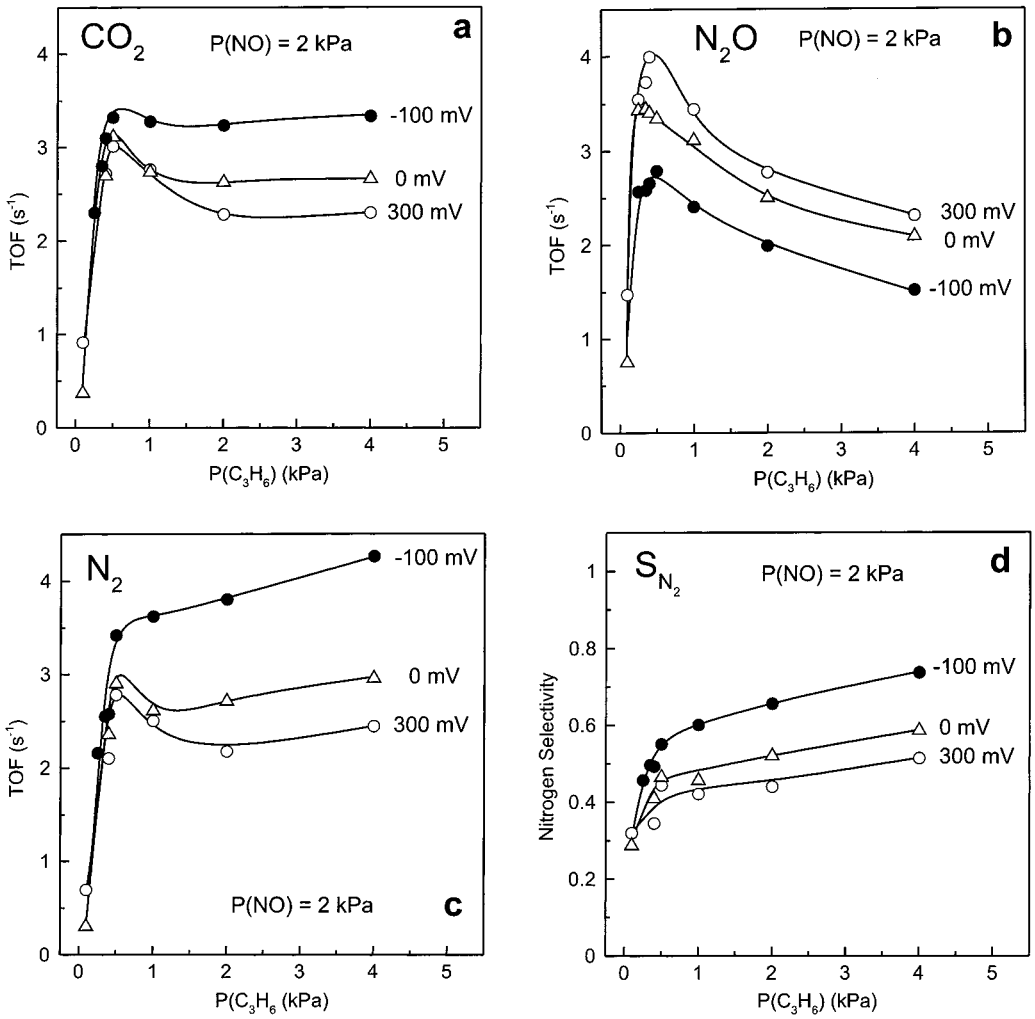

Figure 2. Effect of propene partial pressure on the rates of CO_2 (a), N_2 (b), and N_2O (c) formation, and on nitrogen selectivity (d), for three different fixed catalyst potentials at 623 K and $P(NO) = 2$ kPa.

The same trends in overall catalytic activity and nitrogen selectivity are visible in Figure 1b. Figure 1c shows that the effects of electro-pumping Na decrease as the NO:C_3H_6 ratio is increased, i.e., in this case decreasing V_{WR} causes little change in the CO_2 rate, a small increase in the N_2 rate, and a substantial decrease in the N_2O rate, resulting in a significant increase in the nitrogen selectivity. Figure 1d shows that as the NO:propene ratio increases further, decreasing V_{WR} causes a decrease in *all* reaction rates but still results in an increase in the nitrogen selectivity. Note that the reaction rates over the unpromoted catalyst ($V_{WR} = +300$ mV) increased as the partial pressure of NO is increased from 1 to 4 kPa (Figure 1a−c) at fixed partial pressure of propene. However, further increasing $P(NO)$ to 9 kPa caused the rates to decrease. This is in excellent agreement with the kinetic data discussed below (Figure 3a−c).

In every case the system's behavior was reversible: returning the catalyst potential to +300 mV (Na-free surface) restored the unpromoted reaction rates. It is apparent that the promotional effect increased as the gas composition became more reducing (lower NO:C_3H_6 ratios). This effect is illustrated in Table 1 which shows the ratio (ρ) of the unpromoted ($V_{WR} = +300$ mV) and optimally promoted reaction rates as a function of the NO:C_3H_6 ratio; optimal promotion corresponds to the minimum value of V_{WR} and the highest rates achieved. Also shown in Table 1 is the variation of the unpromoted and optimally promoted values of the S_{N_2} with NO:propene ratio. It is evident that increasing the NO:propene ratio causes: (i) a decrease in all ρ values, and (ii) a decrease in nitrogen selectivity for both the unpromoted and optimally promoted catalyst. These observations are also in good agreement with the kinetic measurements described below.

3.2. Effect of Partial Pressures on Unpromoted and Promoted Reaction Rates. Parts a, b, and c of Figure 2 show the turnover frequencies of CO_2, N_2O, and N_2 production at 623 K for three different values of catalyst potential as a function of propene partial pressure, for a fixed NO partial pressure (2 kPa). Figure 2d shows corresponding results for the nitrogen selectivity. In most cases a rate maximum is observed indicating that the reaction follows Langmuir−Hinshelwood type kinetics reflecting competitive adsorption of the two reactants. It is apparent that as the catalyst potential was decreased to more negative values (increasing the sodium coverage), there was an increase in the CO_2 and N_2 production rates and a decrease in the N_2O rate. This resulted in an increase in nitrogen selectivity over the whole range of partial pressures (Figure 2d). Figure 2d also shows that the nitrogen selectivity of the unpromoted and promoted catalyst increases as the C_3H_6:NO ratio is increased.

Figure 3a−d depicts analogous results for the effect of NO at three different catalyst potentials for a fixed (1 kPa) partial pressure of propene. In this case the Langmuir−Hinshelwood rate maxima were inaccessible within the NO partial pressure range of our experiments, reflecting the weaker adsorption of NO relative to propene. In accord with the catalyst potential

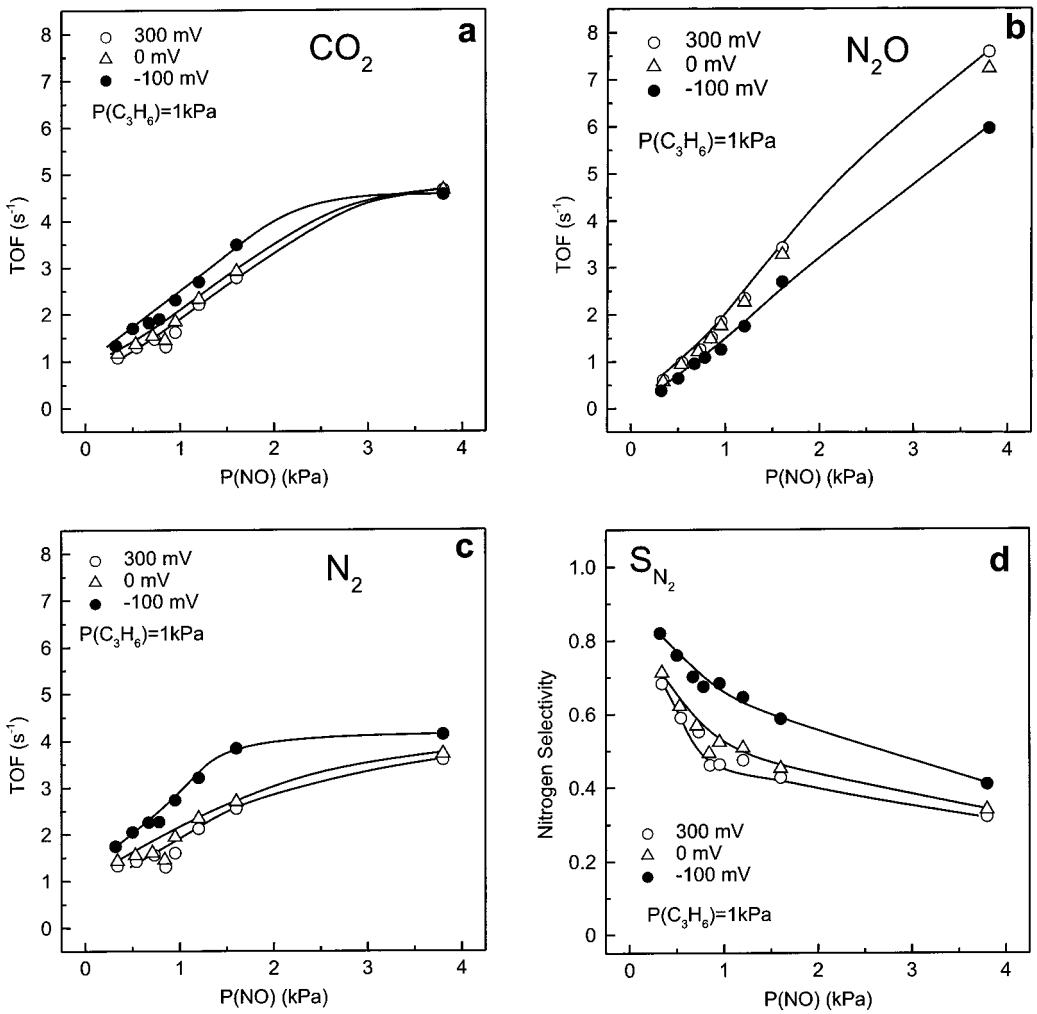

Figure 3. Effect of NO partial pressure on the rates of CO_2 (a), N_2 (b), and N_2O (c) formation, and on nitrogen selectivity (d), for three different fixed catalyst potentials at 623 K and $P(C_3H_6) = 1$ kPa.

TABLE 1: Effect of NO:C_3H_6 Ratio on Reaction Rates and Nitrogen Selectivity[a]

P^0(NO):P^0(C_3H_6)	$\rho(CO_2)$	$\rho(N_2)$	$\rho(N_2O)$	$S^u(N_2) \rightarrow S^p(N_2)$
1 kPa:1 kPa	1.7	2.4	0.4	45% → 82%
2 kPa:1 kPa	1.4	1.9	0.6	36% → 66%
4 kPa:1 kPa	1	1.3	0.5	30% → 51%
9 kPa:1 kPa	0.35	0.5	0.3	22% → 31%

[a] *u*, *p* refer to unpromoted and optimally promoted cases, respectively.

dependence of the reaction rates (Figure 1), Figure 3a−d shows that as the catalyst potential decreased the CO_2 and N_2 rates and nitrogen selectivity increased while the N_2O rate decreased.

A comparison of the trends shown in Figures 2 and 3 indicates that increasing amounts of sodium on the catalyst (decreasing V_{WR}) resulted in an increase in the CO_2 and N_2 formation rates, and a decrease in the N_2O rate. These effects are more pronounced at higher propene:NO ratios, in agreement with the results displayed in Table 1 and described in the previous section. Note also that the nitrogen selectivity of the unpromoted and promoted catalysts decreased as the NO:propene ratio increased (Figures 2d and 3d), in line with the data presented in Table 1.

3.3. Effect of CO_2 Partial Pressure on Reaction Rates. As will be shown in the next section, spectroscopic data suggest that the chemical state of the promoter phase under reaction conditions is sodium carbonate. Therefore we investigated the effect of deliberately adding CO_2 to the reaction mixture. We found that CO_2 addition had no detectable effects.

3.4. X-ray Photoelectron Spectroscopy. XP spectra were obtained immediately after exposing the appropriately biased catalyst film to the conditions of temperature and reactants partial pressures typical of those encountered in the reactor, to determine what stable surface species were present under reaction conditions. During exposure of the catalyst to the reaction mixture, the V_{WR} values were such that the Rh film was either (i) electrochemically clean (+600 mV, unpromoted) or (ii) sodium-promoted (−100 mV). A detailed description of the procedure followed to obtained the postreaction XP spectra can be found in an earlier publication.[10] Spectra were acquired after exposing the sample to a mixture of (1 kPa of propene + 1 kPa of NO), diluted in He, at 623 K, and 1 bar total pressure. In every case Na 1s, Rh 3d, C 1s, O 1s, N 1s XP spectra were obtained under the following four sets of conditions: (i) after exposing the unpromoted sample to reaction gas (spectrum a); (ii) after exposing the promoted sample to reaction gas (spectrum b); (iii) after heating the postreaction promoted sample in UHV at 623 K under open circuit conditions (spectrum c); and finally (iv) after cleaning the surface by imposing a positive bias (V_{WR} = +600 mV) at 623 K (spectrum d). Spectra a and b were acquired at room temperature under open circuit conditions; spectrum c at 623 K, open circuit; spectrum d at 623 K and +600 mV.

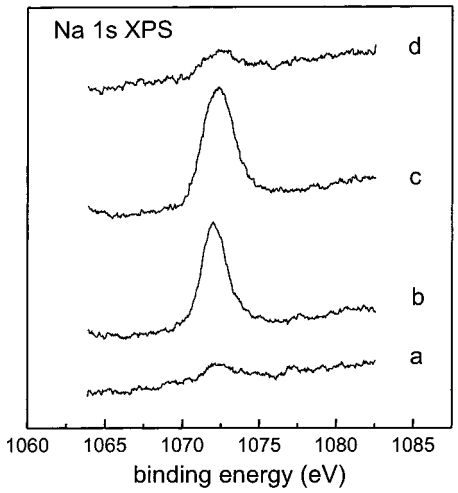

Figure 4. Na 1s XP spectra acquired after exposure to (1 kPa of propene + 1 kPa of NO) at 623 K with $V_{WR} = +600$ mV (a) and with $V_{WR} = -100$ mV (b). Spectrum (c) was acquired after spectrum (b) by heating to 623 K. Spectrum (d) was taken after heating at 623 K with $V_{WR} = +600$ mV.

Figure 4 shows the resulting Na 1s XP spectra for each of the four conditions described above. Within the sampling depth of the technique (~5 Å, photoelectron kinetic energy 180 eV), a small amount of sodium was detected after exposing the sample to the reaction mixture under unpromoted conditions (spectrum a). We have previously shown that this residual Na signal is due to sodium in the β''-alumina electrolyte which is spectroscopically visible through the cracks and imperfections in the porous rhodium film.[7,9,11] The postreaction promoted sample ($V_{WR} = -100$ mV) exhibits a much larger Na 1s signal (spectrum b). Heating the promoted sample to 623 K increased the Na 1s intensity and broadened the peak to higher binding energy (spectrum c). These changes, which reflect a change in the nature of the sodium promoter phase, can be correlated with corresponding changes in the C1s and O1s emission, as discussed below. Electrochemical cleaning (catalyst potential held at +600 mV) caused a large decrease in Na 1s intensity, resulting in a spectrum essentially identical to spectrum a.

Rh 3d XP spectra are shown in Figure 5. Two points should be noted. First, the BE and line shape are invariant, indicating that there was no oxidation of the rhodium film under any conditions. The second point concerns the degree of intensity attenuation which provides a measure of the amount of material present on the surface. For purposes of comparison the clean surface spectrum taken before any exposure of the catalyst to reaction gas is also shown (labeled "initial"). After exposing unpromoted sample reaction gas the Rh XPS signal was attenuated by 13%. This corresponds to a uniform layer of material ~2.6 Å thick covering about half the Rh surface (photoelectron escape depth = 11.62 Å[12]). A substantial increase in attenuation of the Rh signal was observed when the promoted sample was exposed to reaction gas (spectrum b). The attenuation of 53% corresponds to a uniform layer of material ~7 Å thick covering the entire Rh surface. Spectrum d was acquired after heating and electrochemically cleaning the surface: note that the Rh signal recovered its initial intensity indicating complete removal of the alkali promoter phase. This is in agreement with the behavior of the Na 1s emission, as discussed above, the C 1s, O 1s, and N 1s emission as discussed below, and with the reactor data presented above.

Carbon 1s XP spectra provide information about the chemical identity of the Na compound(s) that are formed under reaction

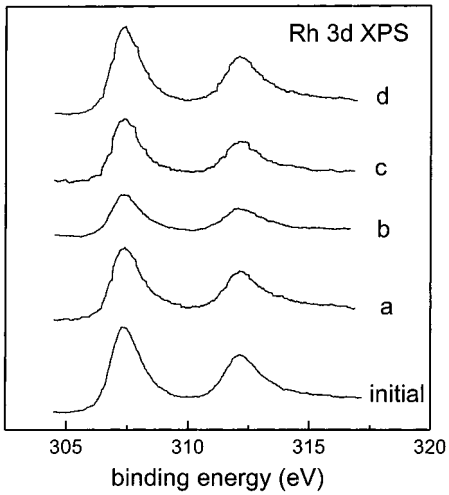

Figure 5. Rhodium 3d XP spectra acquired before exposing the sample to the reaction mixture (initial) and after exposure to (1 kPa of propene + 1 kPa of NO) at 623 K with $V_{WR} = +600$ mV (a) and with $V_{WR} = -100$ mV (b). Spectrum (c) was acquired after spectrum (b) by heating to 623 K. Spectrum (d) was taken after heating at 623 K with $V_{WR} = +600$ mV.

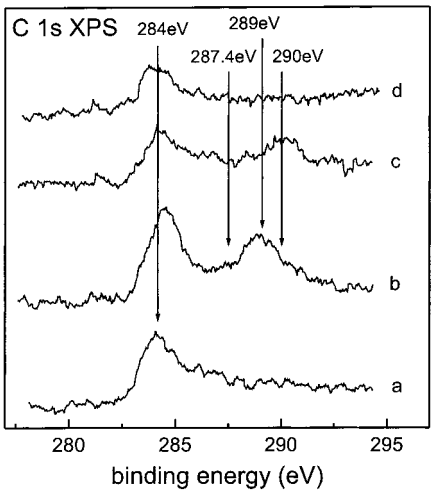

Figure 6. Carbon 1s XP spectra acquired after exposure to (1 kPa of propene and 1 kPa of NO at $T = 623$ K with $V_{WR} = +600$ mV (a) and with $V_{WR} = -100$ mV (b). Spectrum (c) was acquired after spectrum (b) by heating to 623 K. Spectrum (d) was taken after heating at 623 K with $V_{WR} = +600$ mV.

conditions (Figure 6). These data suggest that Na is present on the surface of the working catalyst as a carbon-containing compound or compounds. The C 1s region comprises two principal features, one at lower BE(~284−285 eV) and the other at higher BE (~288−290 eV). The former is due to elemental carbon (284 eV[13]) and propene fragments (284−285 eV), whereas the latter corresponds to sodium carbonate (289 eV[14]). Exposure of the unpromoted catalyst to reaction gas (spectrum a) led to the appearance of a broad poorly resolved feature containing at least two components: (i) elemental carbon at 284 eV and (ii) propene fragments at 284−285 eV. Exposing the promoted catalyst to reaction mixture (spectrum b) caused the appearance of at least four features, as follows: (i) elemental carbon at 284 eV, (ii) propene fragments at 284−285 eV, (iii) a small but reproducible shoulder at 287.4 eV which may be due to partially oxidized propene fragments,[13] and (iv) a peak at 289 eV due to sodium carbonate. Heating this sample to 623 K under UHV and open circuit conditions resulted in spectrum c which exhibits the same low binding energy features as

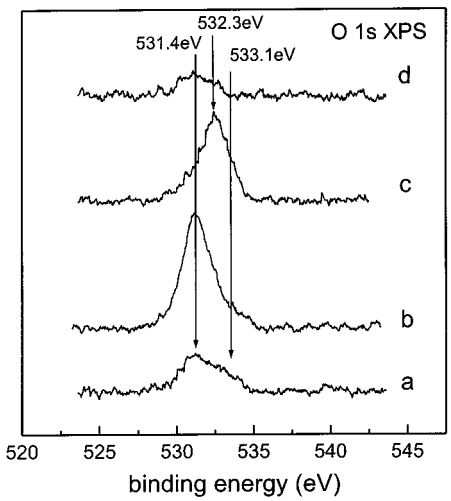

Figure 7. Oxygen 1s XP spectra acquired after exposure to (1 kPa of propene + 1 kPa of NO) at 623 K with $V_{WR} = +600$ mV (a) and with $V_{WR} = -100$ mV (b). Spectrum (c) was acquired after spectrum (b) by heating to 623 K. Spectrum (d) was taken after heating at 623 K with $V_{WR} = +600$ mV.

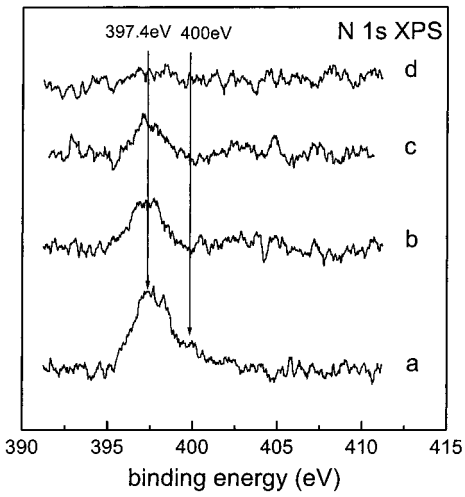

Figure 8. Nitrogen 1s XP spectra acquired after exposure to (1 kPa of propene + 1 kPa of NO) at 623 K with $V_{WR} = +600$ mV (a) and with $V_{WR} = -100$ mV (b). Spectrum (c) was acquired after spectrum (b) by heating to 623 K. Spectrum (d) was taken after heating at 623 K with $V_{WR} = +600$ mV.

spectrum b (284 eV and 284−285 eV). However, there are two differences: (i) the peak at 287.4 eV is absent in spectrum c , and (ii) the peak at 289 eV in spectrum b is replaced by a much smaller peak at 290 eV in spectrum c. The latter changes correlate with the changes observed in the Na 1s and O 1s regions, shortly to be described. Finally, setting V_{WR} to +600 mV (thus pumping Na away from the surface) caused the disappearance of 290 eV peak leaving only a very small amount of elemental carbon on the surface (spectrum d) in accord with the corresponding changes in the Rh 3d, O 1s, and Na 1s regions.

The O 1s spectral region (Figure 7) contains three principal contributions. The lower BE peak is due to chemisorbed oxygen (531.4 eV[15]) and carbonate (531.6 eV[16]). The intermediate BE peak (532.3 eV) must be associated with a sodium compound since it disappears under positive bias. The highest BE peak (533.1 eV) has previously been attributed to subsurface oxygen by Tolia et al.[15]

On the above basis we may make the following assignments. Exposing the unpromoted catalyst to reaction conditions generates chemisorbed oxygen and subsurface oxygen (spectrum a). Exposing the Na-promoted catalyst reaction conditions generates chemisorbed oxygen, sodium carbonate, and subsurface oxygen. Heating this surface under open circuit conditions results in a dramatic change in the O 1s spectrum which correlates with changes in the Na 1s line shape and in the C 1s intensity and BE. Finally, cleaning the surface by applying a $V_{WR} = +600$ mV resulted in the disappearance of the O 1s emission due to sodium carbonate, leaving only a small amount of chemisorbed oxygen on the surface.

Figure 8 shows the corresponding N 1s XP spectra. Two main features are readily distinguished: (i) chemisorbed N at 397.4 eV,[17] and (ii) chemisorbed NO at 400 eV.[18] That is, exposing the unpromoted sample to reaction conditions resulted in the presence of both chemisorbed N and NO (spectrum a). However, when the sample was promoted with Na, only chemisorbed N was detected (spectrum b).

4. Discussion

The effects of controlled variations in Na loading on the catalytic behavior of the rhodium film may be summarized as follows:

(i) Sodium causes an increase in the rate of CO_2 and N_2 formation for $P(NO)/P(C_3H_6) < 4$.

(ii) Sodium causes a decrease in the N_2O production rate.

(iii) Sodium causes an increase in the nitrogen selectivity under all the conditions explored.

Figures 1−3 and Table 1 show that the effectiveness of sodium promotion is strongly dependent on gas-phase composition. The clean surface rate increased and the effect of sodium decreased as the NO:propene ratio increased (Figure 3). Correspondingly, the promotional effect of sodium increased as the NO:propene ratio decreased (Figure 2). These observations provide a strong indication as to the mode of action of the electro-pumped Na in promoting the reduction of NO by propene. As discussed below and suggested earlier in connection with our work on EP of the CO + NO reaction over Pt[19] and Rh[7] and of the NO + C_3H_6 reaction over Pt,[11] we propose that the promotional effect is due to enhanced NO chemisorption and dissociation induced by electrochemically pumped sodium. NO dissociation triggers the reaction by producing the O_a species responsible for initiating the ensuing oxidation reactions of adsorbed propene and propene fragments. The way in which Na enhances the strength of NO adsorption and decreases the activation energy to its dissociation is well understood theoretically;[20] it has also been demonstrated experimentally (see for example refs 21−24).

The dependence of activity and selectivity on catalyst potential for different NO:propene ratios may be rationalized by considering the relative effect of Na on the surface chemistry of coadsorbed propene and NO. For low NO:propene ratios and at high positive potential the Rh surface is free of sodium (Figure 4, spectrum a) and covered mainly with propene. As the catalyst potential is decreased (pumping Na to the Rh surface), the electronic effect of the sodium promoter strengthens the Rh−N bond (increasing NO coverage) and weakens the N−O bond (facilitating NO dissociation). Thus, the effect of the promoter is to enhance surface coverage by NO and its dissociation products. Our XPS data provide evidence in support of this view. Thus a comparison of spectra a and b in Figure 7 shows that the amount of chemisorbed oxygen (produced by NO dissociation) is greater when sodium is present on the catalyst. Strong corroboration is provided by spectra a and b in Figure 8 which

show that NO is only detected on the rhodium surface only when there is no Na present.

Sodium also enhances the selectivity toward N_2 formation. This quantity is determined by the competition between the following surface reactions:

$$NO(a) + N(a) \rightarrow N_2O(g) + 2S \quad (1)$$

$$N(a) + N(a) \rightarrow N_2(g) + 2S \quad (2)$$

Where S represents a vacant site for adsorption and a (g) stands for adatom (gas). The observed increase in selectivity is a consequence of the Na-induced decrease and increase, respectively, in the amounts of molecularly adsorbed NO and atomic N on the surface, thus favoring the first reaction over the second. Qualitatively similar effects on nitrogen selectivity have been found for the sodium-promoted NO reduction by CO[7,19] and propene.[11]

As noted above, the promotional effect of Na diminished as the NO:propene ratio increased. For example, Figure 1d shows that at NO:propene = 9, decreasing the catalyst potential (increasing the sodium coverage) resulted in a decrease of all reaction rates. This may be understood in terms of the effect of sodium on the competitive adsorption of the reactants. Alkali decreases the chemisorption strength of propene (an electron donor) while enhancing the chemisorption of NO (an electron acceptor). Under reducing conditions (low NO:propene), self-poisoning due to excessive adsorption of propene and its decomposition products *can* be counteracted by the opposite effects of alkali on the adsorption of NO and propene. However, as the NO:propene ratio is increased beyond a certain point, alkali-enhanced adsorption of NO swamps NO adsorption and the system now self-poisons for the opposite reason, resulting in the observed decrease in reaction rates.

The key assumption underlying much of the preceding discussion is that changes in V_{WR} result in reversible pumping of Na to/from the Rh from/to the solid electrolyte. Our XPS data (Figure 4) convincingly demonstrate that such reversible transport of sodium between the solid electrolyte and the gas-exposed surface of the Rh film does indeed occur under the conditions of catalyst potential and temperature used for the reactor studies. This important observation substantiates our view of the mode of action of the EP system: it works by electrochemically controlled spillover or back-spillover of the promoter species between the electrolyte and the metal catalyst. Figure 4 illustrates the direct correspondence between catalyst potential and sodium coverage. It also shows that the processes involved are fully reversible, since the original spectrum is restored upon electrochemically pumping Na away from the Rh surface. This is in excellent agreement with the reversible dependence of reaction rates on catalyst potential.

Controlling the catalyst potential controls the level of sodium promoter on the catalyst. In the presence of a reactive gas atmosphere, the promoter phase must be present as sodium-containing compounds. The XPS data reveal the chemical identity of the principal surface compounds that are present; they also provide some indication of the likely morphology of these compounds.

The Rh 3d XP spectra (Figure 5) are revealing in regard to the extent of loading and morphology of the Na surface compounds. First, recall that the attenuation of Rh 3d emission from the postreaction unpromoted surface corresponds to the presence of about half a monolayer of adsorbed material. That is, the metal surface is extensively covered with N, NO, O, and propene fragments. The analogous data for the promoted catalyst nominally correspond to uniform coverage by a film ~7 Å thick, consisting mainly of the sodium promoter phase. However, since the promoted surface is even more active than the unpromoted surface, it follows that a substantial fraction of the former must consist of active metal sites. Therefore the material contained in the nominal ~7 Å thick layer must be distributed as 3D crystallites on an otherwise bare (promoted) metal surface. In other words our picture of the promoted working catalyst under steady-state conditions is one of gas-exposed Rh sites modified by submonolayer amounts of the alkali promoter in coexistence with areas covered by crystallites of Na promoter compound. The size and distribution of these crystallites cannot of course be inferred from the XPS data; this would require application of an imaging technique and such experiments are planned.

The C 1s and O 1s data shown in Figure 6 (spectrum b) and Figure 7 (spectrum b) provide strong evidence that the promoter phase consists principally, if not entirely, of Na_2CO_3. Heating this promoted surface under UHV conditions results variously in changes of line shape, BE and/or intensity in the Na 1s, C 1s, and O 1s and Rh 3d emission, as described in detail in Section 3.4. Here it is worth recalling that the literature contains a range of BEs for sodium carbonate, depending on the nature of the sample. Quoted C 1s BEs range from 289.4 eV for bulk sodium carbonate[25] to 290.4 eV for submonolayer quantities,[26] the corresponding range for O 1s BEs being 531.6 eV − 532.2 eV. Therefore, we propose that the observed thermally induced changes under vacuum reflect changes in morphology and chemical state of the promoter phase. Thus partial evaporation of 3D crystallites of sodium carbonate to yield thinner structures would account for the observed decrease in C 1s carbonate emission. Interestingly, the Na 1s emission actually increased, suggesting formation of some compound (possibly an oxide of Na) that wets the Rh surface better than carbonate.

The present results are in excellent agreement with our previous work on sodium promotion of NO reduction by propene over conventional dispersed Rh/γ-alumina catalysts.[6] The Na-induced rate gains and selectivity observed with the dispersed catalysts ($\rho(N_2) = 3.3$, $\Delta S = 53\% \rightarrow 90\%$) are entirely comparable with those found here under similar conditions: $\rho(N_2) = 2.4$, $\Delta S = 45\% \rightarrow 82\%$. Furthermore, the decrease in promotion with increasing the NO:propene ratio was also found with the sodium-promoted dispersed catalysts.[6] Therefore we conclude that the mechanistic interpretations offered here also apply to the dispersed Rh catalysts. The EP approach eliminates ambiguities that arise with dispersed catalyst data due to the unknown distribution of the promoter between the metal and support phases. Thus we may infer with some confidence that Na promotion of conventional dispersed Rh catalysts is due to effects on the surface chemistry of the metal component and that effects of the alkali on the support are not significant.

5. Conclusions

(1) Electrochemical promotion of Rh is due to the reversible transport of ions between the solid electrolyte and the metal film catalyst with which it is in contact. The coverage of promoter species is controlled by the catalyst potential, measured with respect to a reference electrode.

(2) In the present case, EP of Rh by Na can greatly enhance its catalytic performance with respect to both activity and nitrogen selectivity in the reduction of NO by propene. These improvements are most pronounced under reducing conditions, decreasing as the NO partial pressure rises. They are unaffected by deliberate addition of CO_2.

(3) Promotion is due to the Na-induced dissociation of NO, the key reaction-initiating step.

(4) Under the reaction conditions, sodium is present as carbonate, some of which is in the form of 3D crystallites.

(5) Comparison of these EP results with corresponding data obtained using conventional dispersed Rh catalysts shows that Na promotion of the practical materials is due to the effects of alkali on the metal surface chemistry. Effects due to alkali on the support must be insignificant.

Acknowledgment. This work was supported by the U.K. Engineering and Physical Sciences Research Council and by the European Union under Grants GR/M76706 and BRPR-CT97-0460, respectively. F.J.W. acknowledges financial support from Fundación YPF, Fundación Antorchas, British Council Argentina and King's College Cambridge.

References and Notes

(1) Taylor, K. C. *Catal. Rev.—Sci. Eng.* **1993**, *35*, 457.
(2) Masel, R. I. *Catal Rev.—Sci Eng.* **1986**, *28*, 335.
(3) Shelef, M.; Graham, G. W. *Catal. Rev.—Sci. Eng.* **1994**, *36*, 433.
(4) Tomishige, K.; Asakura, K.; Iwasawa, Y. *J. Catal.* **1995**, *157*, 472.
(5) Chafik, T.; Efstathiou, A. M.; Verykios, X. E. *J. Phys Chem. B* **1997**, *101*, 7968.
(6) Macleod, N.; Isaac, J.; Lambert, R. M. *J. Catal.* **2000**, *193*, 115.
(7) Williams, F. J.; Palermo, A.; Tikhov, M. S.; Lambert, R. M. *J. Phys. Chem. B* **2000**, *104*, 11883.
(8) Komai, S.; Hattori, T.; Murakami, Y. *J. Catal.* **1989**, *120*, 370.
(9) Williams, F. J.; Palermo, A.; Tikhov, M. S.; Lambert, R. M. *J. Phys. Chem. B* **2000**, *104*, 615.
(10) Williams, F. J.; Palermo, A.; Tikhov, M. S.; Lambert, R. M. *J. Phys. Chem. B* **1999**, *103*, 9960.
(11) Yentekakis, I. V.; Palermo, A.; Filkin, N. C.; Tikhov, M. S.; Lambert, R. M. *J. Phys. Chem. B* **1997**, *101*, 3759.
(12) Penn, D. R. *J. Electron Spectrosc. Relat. Phenom.* **1976**, *9*, 29.
(13) Paal, Z.; Schlogl, R.; Ertl, G. *J. Chem. Soc., Faraday Trans.* **1992**, *88*, 1179 and references therein.
(14) Seyller, Th.; Borgmann, D.; Wedler, G. *Surf. Sci.* **1998**, *400*, 63.
(15) Tolia, A. A.; Smiley, R. J.; Delgass, W. N.; Takoudis, C. G.; Weaver, M. J. *J. Catal.* **1994**, *150*, 56.
(16) Wagner, C. D.; Zatko, D. A.; Raymond, R. H. *Anal. Chem.* **1980**, *52*, 1445.
(17) Baird, R. J.; Ku, R. C.; Wynblatt, P. *Surf. Sci.* **1980**, *97*, 346.
(18) DeLouise, L. A.; Winograd, N. *Surf. Sci.* **1985**, *159*, 199.
(19) Palermo, A.; Lambert, R. M.; Harkness, I. R.; Yentekakis, I. V.; Marina, O.; Vayenas, C. G. *J. Catal.* **1996**, *161*, 471.
(20) Lang, N. D.; Holloway, S.; Norskov, J. K. *Surf. Sci.* **1985**, *150*, 24.
(21) Harkness, I. R.; Lambert, R. M. *J. Chem. Soc., Faraday Trans.* **1996**, *93*, 1425.
(22) Bugyi, L.; Solymosi, F. *Surf. Sci.* **1987**, *188*, 475.
(23) Bugyi, L.; Kiss, J.; Revesz, K.; Solymosi, F. *Surf. Sci.* **1990**, *233*, 1.
(24) Hochst, H.; Colavita, E. *J. Vac. Sci. Technol. A* **1986**, *4*, 1442.
(25) Gelius, U.; Heden, P. F.; Hedman, J.; Lindberg, B. J.; Manne, R.; Nordberg, R.; Nordling, C.; Siegbahn, K. *Phys. Scr.* **1970**, *2*, 70.
(26) Nerlov, J.; Christensen, S. V.; Weichel, S.; Pedersen, E. H.; Moller, P. J. *Surf. Sci.* **1997**, *371*, 321.